THE JOURNAL OF PHYSICAL CHEMISTRY C

ARTICLE

pubs.acs.org/JPCC

SnO_2/Reduced Graphene Oxide Nanocomposite for the Simultaneous Electrochemical Detection of Cadmium(II), Lead(II), Copper(II), and Mercury(II): An Interesting Favorable Mutual Interference

Yan Wei,[†,‡,§] Chao Gao,[†] Fan-Li Meng,[†] Hui-Hua Li,[†] Lun Wang,[*,§] Jin-Huai Liu,[*,†] and Xing-Jiu Huang[*,†]

[†]Institute of Intelligent Machines, Chinese Academy of Sciences, Hefei 230031, People's Republic of China

[‡]Department of Chemistry, Wannan Medical College, Wuhu 241002, People's Republic of China

[§]College of Chemistry and Materials Science, Anhui Normal University, Wuhu 241000, People's Republic of China

ABSTRACT: A well-known gas sensing material SnO_2 in combination with reduced graphene oxide was used in heavy metal ions detection for the first time. This work reports the detailed study on the SnO_2/reduced graphene oxide nanocomposite modified glass carbon electrode, which could be used for the simultaneous and selective electrochemical detection of ultratrace Cd(II), Pb(II), Cu(II), and Hg(II) in drinking water. The SnO_2/reduced graphene oxide nanocomposite electrode was characterized voltammetrically using redox couples ($Fe(CN)_6^{3-/4-}$), complemented with electrochemical impedance spectroscopy (EIS). Square wave anodic stripping voltammetry (SWASV) has been used for the detection of Cd(II), Pb(II), Cu(II), and Hg(II). The detection limit (3σ method) of the SnO_2/reduced graphene oxide nanocomposite modified GCE toward Cd(II), Pb(II), Cu(II) and Hg(II) is 1.015×10^{-10} M, 1.839×10^{-10} M, 2.269×10^{-10} M, and 2.789×10^{-10} M, respectively, which is very well below the guideline value given by the World Health Organization. The chemical and electrochemical parameters that exert influence on deposition and stripping of metal ions, such as supporting electrolytes, pH value, deposition potential, and deposition time, were carefully studied. An interesting phenomenon of mutual interference was observed. Most importantly, we pose a potential for the use of gas sensing material in heavy metal ions detection.

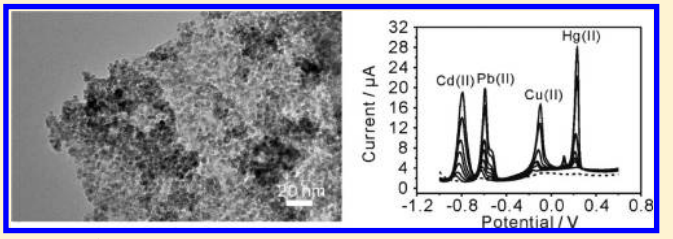

1. INTRODUCTION

Heavy metals are extremely harmful pollutants in the biosphere due to their toxicity and even trace amounts of them pose a detrimental risk to human health. Thus, it is very important to search for a rapid, sensitive, and simple analytical method for the detection and monitoring of these environmental pollutants in water. There are already many mature methods to analyze heavy metal ions, such as atomic absorption spectroscopy, inductively coupled plasma atomic emission spectrometry, and inductively coupled plasma mass spectrometry. However, these spectrometric methods are expensive and not suitable for in situ analysis due to the ponderous and complicated instruments. On the contrary, the electrochemical method, as an alternative to these spectroscopic techniques, has been accepted as an efficient method to detect heavy metal ions due to their excellent sensitivity, short analysis time, portability, and low cost. Among all of the electrochemical methods, electrochemical stripping voltammetric analysis provides a powerful tool for the determination of metal ions, which possess high-sensitivity and can simultaneously analyze several heavy metal ions.[1−5] The use of the chemical modified electrodes tremendously improves the efficiency of accumulating target analytes and has been developed as a fascinating and effective way for the anodic stripping voltammertry determination of heavy metal ions. The nanostructured materials are extremely attractive to modify electrodes for electrochemically detecting heavy metal ions due to their unique electronic, chemical, thermal, and mechanical properties in comparison with conventional materials.[6]

Graphene, as a "star" material, has been developed as an advanced nanoelectrocatalyst for constructing electrochemical sensors owing to its extraordinary electronic transport properties, large surface area, and high electrocatalytic activities.[7] In addition, most of the graphene used in electrochemistry is produced from the reduction of graphene oxide and usually has functional groups such as hydroxyl and carboxyl, which are advantageous for adsorbing heavy metal ions.[8] However, because of the van der Waals and $\pi-\pi$ stacking interactions among individual graphene sheet interactions, the as-reduced graphene sheets tend to form irreversible agglomerates and even restack to form graphite when graphene dispersion solutions are dried.[9−11] By incorporation of nanoparticles into graphene sheets, the aggregation problem of graphene sheets could be minimized or prevented.[12] Recently, graphene-based nanosensors have been fabricated aiming to employ them in electrochemical detecting heavy metal ions, such as graphene decorated with metal nanoparticles[13] and conducting polymer.[14,15] However, very

Received: October 12, 2011
Revised: December 1, 2011
Published: December 07, 2011

few reports on the graphene decorated with metal oxides nanoparticles could be found in electrochemical detecting heavy metal ions.

Tin oxide (SnO_2) is a well-known semiconductor and gas sensing material, and has been used as electrode material.[16] The SnO_2 nanomaterials have been widely studied in the gas sensor[17] and anode material for lithium-ion batteries.[17,18] In addition, there have been a few reports about the preparation of SnO_2/graphene composites with application in gas sensor,[19] lithium batteries,[20,21] and supercapacitors.[22] However, to the best of our knowledge, both SnO_2 and SnO_2/graphene nanocomposites have never been found in heavy metal ion detection. As we know, SnO_2 is an oxide which may adsorb heavy metal ions,[23] and its nanoparticles possess unique properties such as high electrical conductivity and chemical sensitivity.[19] However, the SnO_2 nanoparticles are easy to aggregate, and then it is hard to obtain the best performance of the SnO_2 nanoparticles. Thus, we try to use reduced graphene oxide as template to prevent the SnO_2 nanoparticles from aggregating and try to use SnO_2 nanoparticles combined with reduced graphene oxide in electrochemical detecting heavy metal ions.

Although a lot of papers have been published on electrochemical sensing heavy metal ions, only a few works on the simultaneous and selective electrochemical sensing several target metal ions could be found in the literature. In this work, SnO_2 was used in combination with graphene to fabricate a electrochemical platform for the simultaneous analysis of Cd(II), Pb(II), Cu(II), and Hg(II) in solution by square wave anodic stripping voltammograms (SWASV) for the first time. The SnO_2/reduced graphene oxide nanocomposite composed of 4−5 nm SnO_2 nanoparticles was synthesized by a simple wet chemical method. Herein, the SnO_2 nanoparticles not only prevented the graphene from gathering together but also acted as electrochemical catalyst in detecting heavy metal ions. Thus, the SnO_2/reduced graphene oxide nanocomposite modified glass carbon electrode showed enhanced sensing performance compared with single SnO_2 and single graphene. Meanwhile, most of the papers reported that if a wide potential separation between the stripping peaks in simultaneous analysis of multiple heavy metal ions exists, there is no interference from each other. However, we observed an interesting phenomenon of mutual interference, even though a wide potential separation exists between the stripping peaks.

2. EXPERIMENTAL SECTION

2.1. Chemical Reagents. All reagents were commercially available from Sinopharm Chemical Reagent Co., Ltd. (China) with analytical grade and were used without further purification. Acetate buffer solutions of 0.1 M for different pH were prepared by mixing stock solutions of 0.1 M NaAc and HAc. Phosphate buffer solutions (PBS) of 0.1 M were prepared by mixing stock solutions of 0.1 M H_3PO_4, KH_2PO_4, K_2HPO_4, and NaOH. The water (18.2 MΩ cm) used to prepare all solution was purified with the NANOpureDiamond UV water system.

2.2. Preparation of SnO_2/Reduced Graphene Oxide Nanocomposie. Graphene oxide was first prepared by a modified Hummers' method.[24] Then the SnO_2/reduced graphene oxide nanocomposite was synthesized using the following one-step wet chemical method. Namely, 0.1 g of the dried graphene oxide was added into 500 mL of deionized water (DI water). The obtained mixture was sonicated for 90 min. At the same time, 2.4 g of $SnCl_4 \cdot 5H_2O$ was dissolved into 20 mL of DI water and then 8 mL of the graphene oxide solution was added, in which the concentration of $SnCl_4$ is about 0.24 M. The above mixture was stirred for 5 h and then centrifuged for 5 min at 8000 r min^{-1}. In order to improve the crystallinity of the SnO_2 and remove the residual water molecules and functional groups from the graphene oxide, the product was heated at 500 °C for 2 h under an argon atmosphere. For comparison, the single SnO_2 and reduced graphene oxide were synthesized using the same process except the addition of the aqueous dispersion graphene oxide and $SnCl_4 \cdot 5H_2O$.

2.3. Preparation of Modified Electrode. Ultrasonic agitation (for 5 min) was used to disperse the SnO_2/reduced graphene oxide nanocomposite into alcohol to give a suspension. Prior to the surface modification, the bare glassy carbon electrode (GCE) was polished carefully with 1.0, 0.3 and 0.05 μm alumina powder, respectively, and rinsed with DI water, followed by being sonicated in alcohol and DI water successively and dried under nitrogen. Then, an aliquot of 5 μL of the mixture was coated on the electrode, and then the solvent was evaporated at room temperature to obtain the SnO_2/reduced graphene oxide nanocomposite film modified electrode. For comparison, single SnO_2, graphene oxide, and reduced graphene oxide modified glass carbon electrode were prepared using the same process.

2.4. Cd(II), Pb(II), Cu(II), and Hg(II) Detection. Square wave anodic stripping voltammetry (SWASV) was used for the detection under optimized conditions. Cd, Pb, Cu, and Hg were deposited at the potential of −1.0 V for 120 s by the reduction of Cd(II), Pb(II), Cu(II), and Hg(II) in 0.1 M NaAc-HAc (pH 5.0). The anodic stripping (reoxidation of metal to metal ions) of electrodeposited metal was performed in the potential range of −1.0 to 0.5 V at the following parameters: frequency, 15 Hz; amplitude, 25 mV; increment potential, 4 mV. The simultaneous and selective detection of Cd(II), Pb(II), Cu(II), and Hg(II) has been performed at the same experimental condition.

2.5. Apparatus. Electrochemical experiments were recorded using a CHI 660D computer-controlled potentiostat (ChenHua Instruments Co., Shanghai, China) with a standard three-electrode system. A bare glassy carbon electrode (GCE, diameter of 3 mm) or modified GCE served as a working electrode; a platinum wire was used as a counter-electrode with a saturated Ag/AgCl electrode (ChenHua Instruments Co., Shanghai, P. R. China) completing the cell assembly.

Scanning electron microscopy (SEM) images were obtained with a FEI Quanta 200 FEG field emission scanning electron microscope. Transmission electron microscopy (TEM) and high-resolution TEM (HRTEM) and energy dispersive spectrometer (EDS) analyses were performed using a JEM-2010 microscope equipped with Oxford INCA EDS operated at 200 kV accelerating voltage (Quantitative method: Cliff Lorimer thin ratio section).

3. RESULTS AND DISCUSSION

3.1. Morphologic Characterization of SnO_2/Reduced Graphene Oxide Nanocomposite. Figure 1 shows the TEM images and phase maps of SnO_2/graphene nanocomposite. As seen, a graphene sheet was coated with lots of homogeneous and dense SnO_2 nanoparticles having highly uniform size. Well-arranged crystalline lattice fringes (Figure 1b) suggest a well-crystallized polycrystalline structure of SnO_2 nanoparticles. The adjacent lattice fringe spacing of about 0.345 and 0.267 nm correspond to

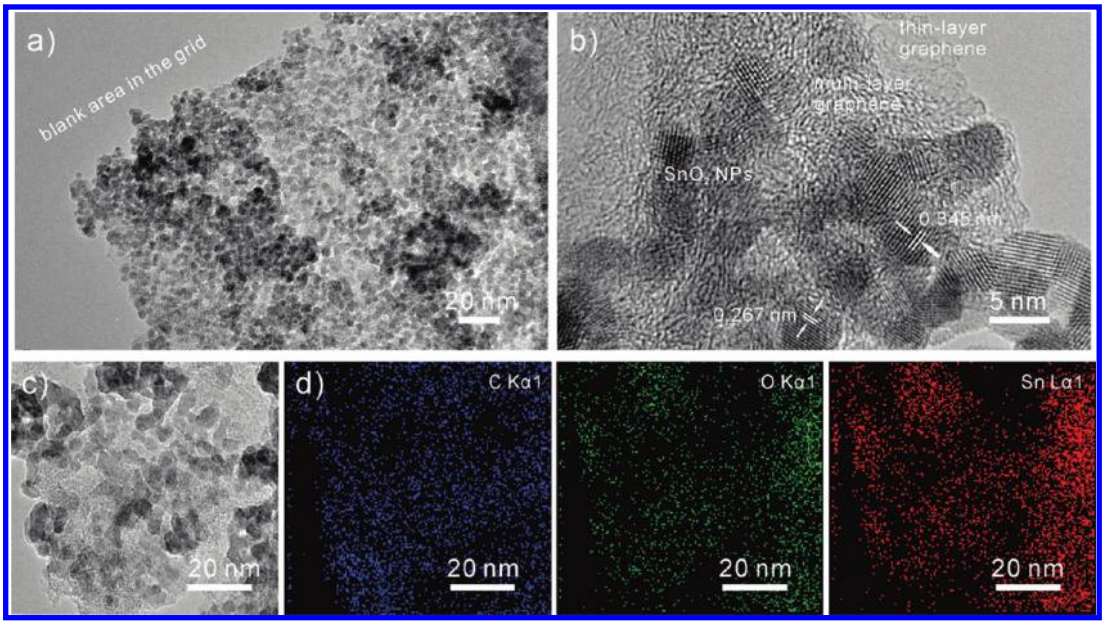

Figure 1. SnO_2/graphene nanocomposite. (a) and (c) TEM images; (b) HRTEM image; and (d) C Kα1, O Kα1, and Sn Lα1 phase maps corresponding to panel c.

the (110) plane and (101) plane of the SnO_2 nanocrystals, respectively.[20,25] The average diameter of the SnO_2 nanoparticles is about 4−5 nm. Further information was obtained from the XRD pattern, XPS, and TGA analysis.[26] The XRD pattern shows that all strong diffraction lines can be indexed to the standard tetragonal SnO_2 phase (JCPDS card no. 41−1445). A calculation using the Scherrer equation gives an average particle size of about 4.3 nm, which is consistent with the observation results from the HRTEM image. The wide-survey XPS spectrum of the SnO_2/graphene nanocomposite suggests the presence of C, O, and Sn. Furthermore, the peaks of Sn and O elements are outstanding and yet the peak of C element is very weak, which suggests the existence of a large amount of SnO_2 nanoparticles. The atomic ratio of C to Sn is about 1:3. In the C 1s spectrum of the SnO_2/graphene nanocomposite, the peak of the C−OH and C−O−C species decreases significantly, which suggests that hydroxyl and epoxy groups reacted with Sn element to form a stannic oxide compound. The content of each component in the prepared nanocomposite can be determined facilely with the TGA technique via oxidative decomposition. It reveals that approximately 90 wt.% of SnO_2 were deposited on the surface of graphene nanosheets. More information about the synthesis and characterization of SnO_2/reduced graphene oxide nanocomposite can be found elsewhere.[26]

3.2. Electrochemical Characterization of SnO_2/Reduced Graphene Oxide Nanocomposite. The cyclic voltammetric response of bare, graphene oxide, reduced graphene oxide, SnO_2 nanoparticle, and SnO_2/graphene nanocomposite modified GCE has been examined using the $Fe(CN)_6^{3-/4-}$ redox couple in neutral solution of 5 mM $Fe(CN)_6^{3-/4-}$ containing 0.1 M KCl (Figure 2). As compared with the bare GCE, the anodic and cathodic peaks almost disappeared at the graphene oxide modified electrode. This is because graphene oxide has many functional groups including hydroxyl and epoxy groups on the planes and carboxyl groups at the edges,[27,28] which block the diffusion of $Fe(CN)_6^{3-}$ to the electrode surface and hinder the electron and mass transfer. On the contrary, reduced graphene oxide modified electrode gives the well-defined peak and higher current, which is attributed to its large 2-D electrical conductivity.[7] In the case of single SnO_2 modified electrode, a similar current response was observed compare with the bare GCE, whereas the peak separations increased obviously. This result indicates that the rate of electron transfer at the electrode surface is hindered with the attachment of SnO_2 to GCE surface. After modifying the SnO_2/reduced graphene oxide nanocomposite, the electrode shows the highest current. This reveals that the combination of SnO_2 and reduced graphene oxide may provide the necessary conduction pathways on the electrode surface and a better electrochemical catalytic behavior, resulting in the promotion of electron transfer process at the modified electrode surface. The cyclic voltammograms of SnO_2/reduced graphene oxide electrode is also observed with huge capacitive current compared with other electrodes. This result is consistent with the previous report, which proves the potential application of SnO_2/reduced graphene oxide nanocomposite in electrochemical supercapacitors.[22]

An electrochemical impedance spectrum (EIS) was employed to further characterize the interface properties of the modified electrodes. In a typical Nyquist plot, the semicircle portion correspond to the electron-transfer resistance (R_{et}) at higher frequency range, while a linear part at lower frequency range represents the diffusion limited process.[29] As seen in the inset of Figure 2, the R_{et} value is about 200 Ω corresponding to the bare GCE. After modification with SnO_2/reduce graphene oxide nanocomposite, the semicircle domain with R_{et} value further decreased and displayed an almost straight line, suggesting the promotion of electron transfer process at the modified electrode surface. These results were supported by the above cyclic voltammogram data.

Figure 3 presents the SWASV analytical characteristics of bare, graphene oxide, reduced graphene oxide, SnO_2 nanoparticle, and SnO_2/reduced graphene oxide modified GCE. When the accumulation process was carried out for 120 s at −1.0 V in a solution containing 0.5 μM each of Cd(II), Pb(II), Cu(II), and Hg(II) in 0.1 M acetate buffer (pH 5.0) without deaeration, nearly no

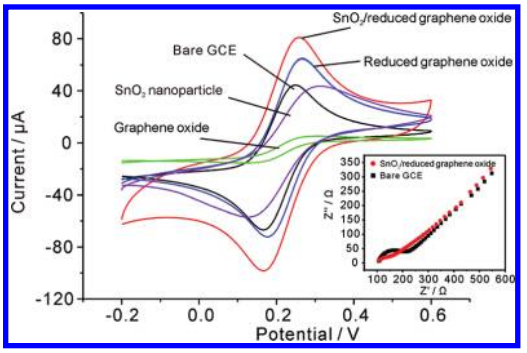

Figure 2. Cyclic voltammograms measured with bare, graphene oxide, reduced graphene oxide, SnO_2 nanoparticle, and SnO_2/reduced graphene oxide nanocomposite modified GCE in the solution of 5 mM $Fe(CN)_6^{3-/4-}$ containing 0.1 M KCl. Inset: Nyquist diagram of electrochemical impedance spectra for bare and SnO_2/reduced graphene oxide nanocomposite modified GCE in the solution of 5 mM $Fe(CN)_6^{3-/4-}$ containing 0.1 M KCl.

peaks at bare (violet line) or reduced graphene oxide (red line) modified GCE, and very weak peaks at SnO_2 nanoparticle (blue line) modified GCE were observed in the potential range of −1.0 to +0.5 V. The sharper and higher peak current for the four target metal ions were obtained at the SnO_2/reduced graphene oxide nanocomposite electrode (pink line). The increase in stripping currents at this modified electrode demonstrates that the SnO_2/reduced graphene oxide nanocomposite is very suitable for the accumulation process of Cd(II), Pb(II), Cu(II), and Hg(II) on the electrode surface (Individually, Cd(II), Pb(II), Cu(II), and Hg(II) can be identified at potentials of −0.774, −0.578, −0.109, and 0.24 V, respectively), resulting in an increased sensitivity. Although strong peak for Cd(II) and Pb(II) were obtained at graphene oxide modified GCE due to lots of functional groups acting as anchor sites to adsorb heavy metal ions on graphene oxide surface, we found that it was very hard to desorb the target metal ions, so pure graphene oxide modified electrode cannot be reused conveniently, thus not suited for implication in practice. Again, in contrast to SnO_2/reduced graphene oxide nanocomposite (pink line) modified GCE, four very weak peaks could be seen at SnO_2 nanoparticle modified electrode. This fact demonstrates that SnO_2 nanoparticles play an important role in reoxidizing metal. The weak response is likely due to the large size of SnO_2 nanoparticle (that is, small size of SnO_2 nanoparticle is unstable which may easily congregate together and grows larger by Ostwald ripening to form a compact film under heating conditions[30]).

3.3. Optimization of Experimental Conditions. In order to get the maximum sensitivity for trace heavy metal detection with SnO_2/reduced graphene oxide nanocomposite modified GCE, the voltammetric parameters (supporting electrolytes, pH value, deposition potential, and deposition time, etc.) were optimized in solution containing 0.5 μM each of Cd(II), Pb(II), Cu(II) and Hg(II). For clarity, we chose Cd(II) and Cu(II) as the typical ions to optimize pH value, deposition potential, and deposition time. Figure 4a reveals the voltammetric behavior to four target metal ions at pH 5.0 in three different supporting electrolytes: 0.1 M NH_4Cl-HCl, phosphate buffer, and acetate buffer. Only three peaks were observed in NH_4Cl-HCl solution and phosphate buffer solution, the peak of Pb(II) could not be observed. However, the well-defined voltammetric peak shapes were observed for all four target metal ions in acetate buffer solution.

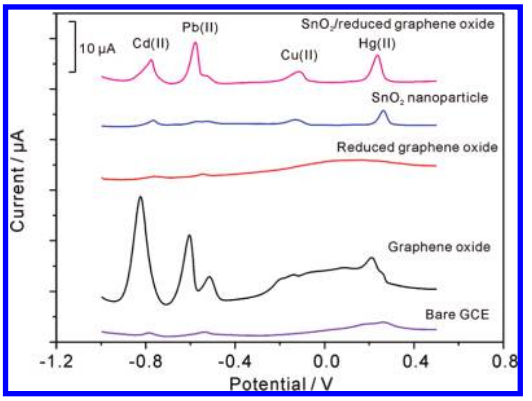

Figure 3. SWASVs for 0.5 μM each of Cd(II), Pb(II), Cu(II), and Hg(II) on bare (violet line), graphene oxide (black line), (c) reduced graphene oxide (red line), (d) SnO_2 nanoparticle (blue line), and SnO_2/reduced graphene oxide nanocomposite (pink line) modified GCE in 0.1 M acetate buffer (pH 5.0). Deposition potential, −1.0 V; deposition time, 120 s; amplitude, 25 mV; increment potential, 4 mV; frequency, 15 Hz; vs Ag/AgCl.

Thus 0.1 M acetate buffer solution, adjusted to pH 5.0, was employed in further experiments.

The effect of pH value is very important and is essential to select a proper pH value. The effect of pH on the voltammetric response was investigated in the pH range 3.0 to 6.0 in 0.1 M acetate buffer solution. As shown in Figure 4b, the peak current for Cd(II) increased as the pH was changed from 3.0 to 5.0, reaching a maximum at pH 5.0, and then decreased up to pH 6.0. For Cu(II), the peak current increased significantly as the pH was changed from 3.0 to 5.0 and then increased slightly up to pH 6.0. It is suggested that the increase in peak current when the pH was changed from 3.0 to 5.0 is due to the electrostatic attraction and complexation mechanism. We believe that the carboxylic and hydroxyl groups acting as anchor sites to adsorb heavy metal ions on graphene surface are similar to those on carbon nanotubes surface, which probably have p*K*a values ranging from 3 to 5.[31] The decrease of the stripping signal for Cd(II) and the slight increase of the stripping signal for Cu(II) at higher pH 6.0 may be related with the hydrolysis of metal ions. Thus, a pH of 5.0 in 0.1 M acetate buffer solution was selected for stripping measurements.

In stripping analysis, the application of adequate deposition potential is very important to achieve the best sensitivity. Thus, the effect of the deposition potential on the peak current after 120 s accumulation was studied in the potential range from 0 to −1.4 V in 0.1 M acetate buffer solution at pH 5.0. The obtained results are shown in Figure 4c. When the deposition potential shifts from 0 to −1.0 V, the stripping peak currents for Cd(II) and Cu(II) increased, and the peak current for Cu(II) reached a maximum at potential −1.0 V. When a deposition potential more negative than −1.0 V was employed, a decrease on the response was observed for Cd(II) and Cu(II). Although a higher peak current for Cd(II) was obtained at an even more negative potential at −1.4 V, to avoid the competitive generation of H_2 and the codeposition of other metal ions from analysis of real samples, we choose −1.0 V as the optimal deposition potential for the subsequent experiment. The difference observed for different metals may be attributed to the different standard potentials.

As the deposition time can affect the detection limit and the sensitivity, different deposition times were studied in this work.

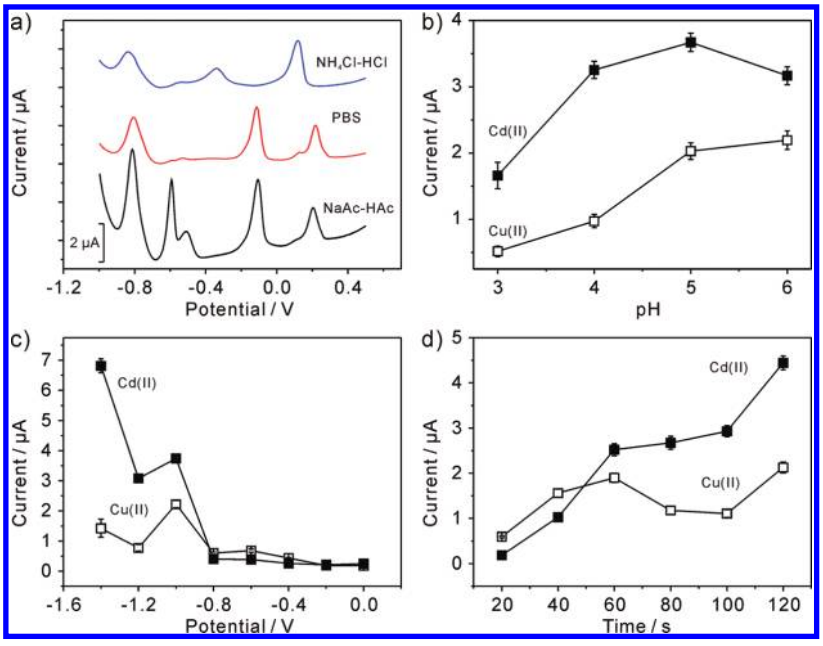

Figure 4. Optmum experimental conditions. Influence of (a) supporting electrolytes; (b) pH value; (c) deposition potential; and (d) deposition time on the voltammetric response of the SnO_2/reduced graphene oxide nanocomposite modified GCE. Data were evaluated by SWASV of 0.5 μM each of Cd(II), Pb(II), Cu(II), and Hg(II). For (b), (c), and (d), Cd(II) and Cu(II) were chosen as the typical ions to show the optimization of the experimental parameters. SWASV conditions are identical to those in Figure 3.

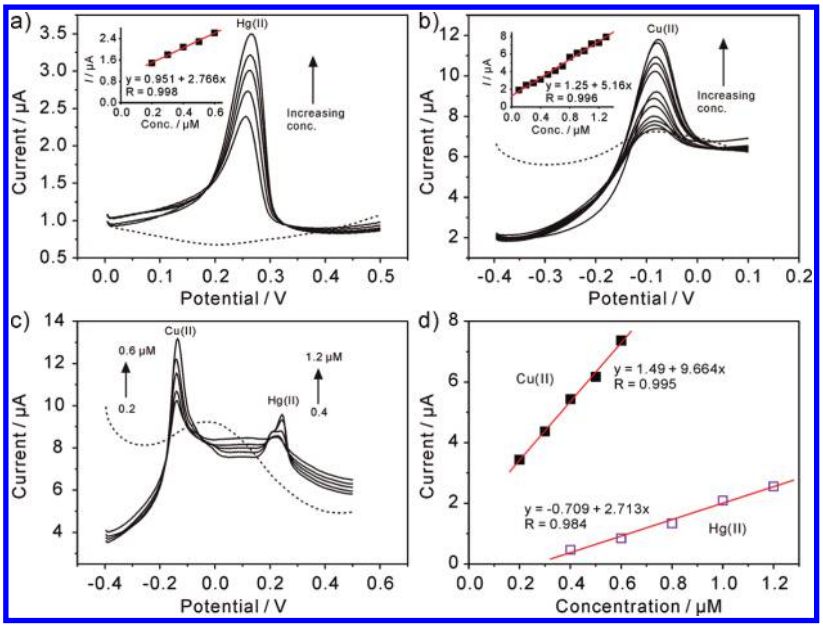

Figure 5. SWASV response of the SnO_2/reduced graphene oxide nanocomposite modified GCE for the individual analysis of (a) Cu(II) over a concentration range of 0.2 to 0.6 μM and (b) Hg(II) over a concentration range of 0.1 to 1.3 μM. Each addition increased the concentration by 0.1 μM. Inset in panel a and b is corresponding linear calibration plot of peak current against Cu(II) and Hg(II) concentrations, respectively. (c) SWASV response of the SnO_2/reduced graphene oxide nanocomposite modified GCE for the simultaneous analysis of Cu(II) and Hg(II) over a concentration range of 0.2 to 0.6 μM for Cu(II) and 0.4 to 1.2 μM for Hg(II). Each addition increased the concentration of Cu(II) by 0.1 μM and Hg(II) by 0.2 μM. (d) The respective calibration curves of Cu(II) and Hg(II) corresponding to panel c. Supporting electrolyte, 0.1 M acetate buffer (pH 5.0); SWASV conditions are identical to those in Figure 3. The dotted line refers to the baseline.

The dependence of peak currents on the deposition time for four target metal ions was depicted in Figure 4d, the response of the stripping peak currents of Cd(II) and Cu(II) enhanced with the increase of the deposition time varying from 20 up to 120 s, this is due to the increased amount of analytes on the modified electrode surface. Although increasing the deposition time improves the sensitivity, it also lowers the upper detection limit due to the surface saturation at high metal ions concentrations.[32] Therefore, to achieve a lower detection limit and wider response range, 120 s was chosen as the deposition time.

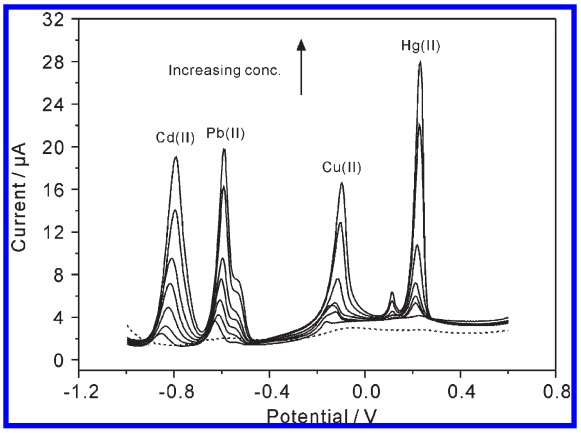

Figure 6. SWASV response of the SnO_2/reduced graphene oxide nanocomposite modified GCE for the simultaneous analysis of Cd(II), Pb(II), Cu(II), and Hg(II) over a concentration range of 0 to 1.3 μM for each metal ions. From bottom to top, 0, 0.3, 0.4, 0.5, 0.6, 0.7, 0.9, and 1.2 μM. SWASV conditions are identical to those in Figure 3.

3.4. Stripping Behavior toward Cd(II), Pb(II), Cu(II), and Hg(II). Under the optimal experimental conditions, Cu(II) and Hg(II) were determined individually and simultaneously at the SnO_2/reduced graphene oxide electrode using SWASV. Figure 5a shows the SWASV responses toward Hg(II) at different concentrations. Well-defined peaks, proportional to the concentration of Hg(II), were observed in the range of 0.2 to 0.6 μM. The linearization equations were $i/\mu A = 0.951 + 2.766c/\mu M$, with the correlation coefficients of 0.998 (inset of Figure 5a). The limit of detection (LOD) was calculated to be 3.438×10^{-11} M (3σ method). The SWASV responses of the SnO_2/reduced graphene oxide electrode toward Cu(II) over a concentration range of 0.1 to 1.3 μM was shown in Figure 5b. The linearization equation was $i/\mu A = 1.25 + 5.167c/\mu M$, with the correlation coefficient of 0.996 (inset of Figure 5b) and with the LOD of 1.141×10^{-10} M (3σ method). When analyzing Cu(II) and Hg(II) simultaneously, as shown in Figure 5c, well-defined peaks of Cu(II) were observed. However, the poor shape of the Hg(II) stripping peaks were also observed. This result was probably due to the formation of Cu−Hg intermetallic compound.[33,34] The resulting calibration plots, as shown in Figure 5d, are linear over the range from 0.2 to 0.6 μM and 0.4 to 1.2 μM for Cu(II) and Hg(II), respectively. The linearization equations were $i/\mu A = 1.49 + 9.664c/\mu M$ and $i/\mu A = 0.709 + 2.713c/\mu M$, with the correlation coefficients of 0.995 and 0.984, respectively. The LOD were calculated to be 3.390×10^{-11} M for Cu(II) and 1.220×10^{-10} M for Hg(II).

The typical records of SWASV analysis for the simultaneous analysis of Cd(II), Pb(II), Cu(II), and Hg(II) at increasing concentrations by SnO_2/reduced graphene oxide nanocomposite electrode under the optimal experimental conditions are displayed in Figure 6. The proposed nanocomposite was successfully applied to the simultaneous determination of the four target metal ions. It shows individual peaks at approximately −0.8, −0.6, −0.1, and 0.24 V for Cd(II), Pb(II), Cu(II), and Hg(II), respectively, in their coexistence. The weak peak obtained between the Cu(II) and Hg(II) was probably due to the formation of intermetallic compound, which have been reported in previous work.[33−39] The separation between the voltammetric peaks is large enough, and hence the simultaneous or the selective detection using the SnO_2/reduced graphene oxide nanocomposite electrode

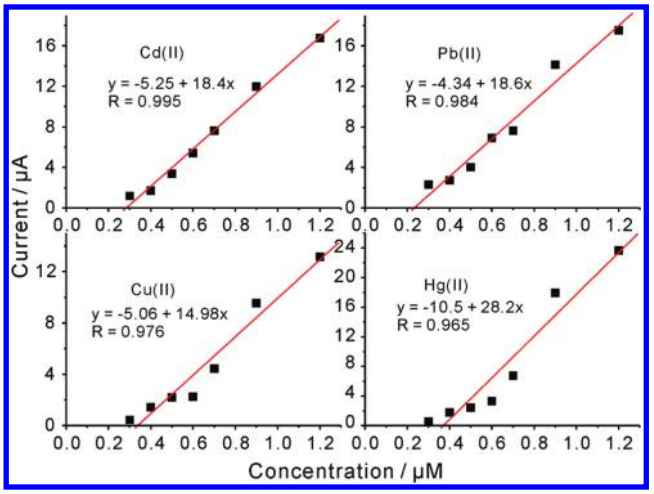

Figure 7. The respective calibration curves of Cd(II), Pb(II), Cu(II), and Hg(II) corresponding to Figure 6.

Table 1. Comparison of Sensing Performance during Individual and Simultaneous Measurements

	analyte	LOD (nM)	correlation coefficient	sensitivity (μA μM^{-1})
individual	Cu(II)	0.1141	0.996	5.167
analysis	Hg(II)	0.03438	0.998	2.766
simultaneous	Cu(II)	0.03390	0.995	9.664
analysis	Hg(II)	0.1220	0.984	2.713
simultaneous	Cd(II)	0.1015	0.995	18.4
analysis	Pb(II)	0.1839	0.984	18.6
	Cu(II)	0.2269	0.976	14.98
	Hg(II)	0.2789	0.965	28.2

is feasible. As shown in Figure 7, the corresponding calibration curves for Cd(II), Pb(II), Cu(II), and Hg(II) were built from 0.3 μM up to 1.2 μM. The linearization equations were $i/\mu A = -5.25 + 18.4c/\mu M$, $i/\mu A = -4.34 + 18.6c/\mu M$, $i/\mu A = -5.06 + 14.98c/\mu M$ and $i/\mu A = -10.5 + 28.2c/\mu M$ for Cd(II), Pb(II), Cu(II) and Hg(II) respectively, with the corresponding correlation coefficients of 0.995, 0.984, 0.976 and 0.965, respectively. The results obtained for LOD were found to be 1.015×10^{-10} M, 1.839×10^{-10} M, 2.269×10^{-10} M and 2.789×10^{-10} M, respectively. These obtained LOD are very well below the guideline value given by the World Health Organization (WHO).

Although the sensing properties of LOD and sensitivity at the SnO_2/reduced graphene oxide nanocomposite were not the best compared with some work reported previously, the modified electrode described here can provide simultaneous analysis of four target heavy metal ions. And the obtained sensing performance is good enough for implication in practice (that is, the excessive high sensitivity may cause unwanted interference and misdetecting). We also found that the SnO_2/reduced graphene oxide nanocomposite electrode can be used repeatedly without regenerating or reactivating the surface between successive determinations and can also be used for a long total experimental time.

3.5. Evaluation of Mutual Interferences. Significant differences in terms of sensitivity were observed when comparing individual with simultaneous analysis (see Table 1). During

dx.doi.org/10.1021/jp209805c |J. Phys. Chem. C 2012, 116, 1034–1041

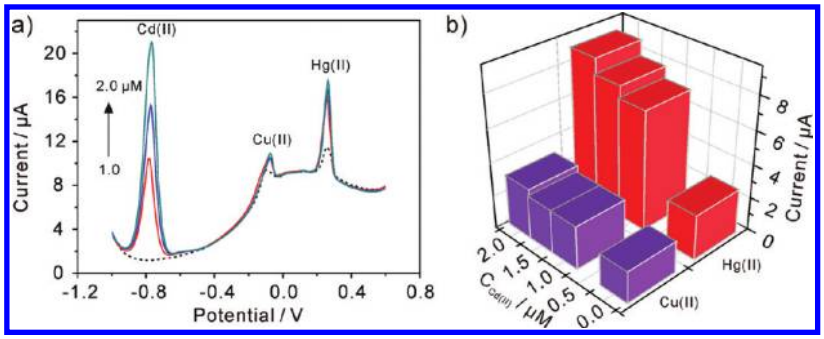

Figure 8. (a) SWASV response of the SnO_2/reduced graphene oxide nanocomposite modified GCE at 0, 1.0, 1.5, and 2.0 μM Cd(II) in the presence of 0.5 μM Cu(II) and 0.5 μM Hg(II) in 0.1 M NaAc-HAc (pH 5.0), showing the interference of the concentrations of Cd(II) on the anodic peak currents of 0.5 μM Cu(II) and 0.5 μM Hg(II). (b) Comparison of the voltammetric peak current of Cu(II) and Hg(II) at different concentrations of Cd(II) corresponding to panel a. SWASV conditions are identical to those in Figure 3.

individual analysis of Cu(II) and Hg(II), the sensitivity obtained were 5.167 $\mu A\,\mu M^{-1}$ for Cu(II) and 2.766 $\mu A\,\mu M^{-1}$ for Hg(II). However, during simultaneous analysis of Cu(II) and Hg(II), the sensitivity obtained were 9.664 and 2.713 $\mu A\,\mu M^{-1}$, respectively. From the data, we find that the sensitivity of Hg(II) almost remains unchanged, whereas the sensitivity of Cu(II) significantly increased. This result is probably due to the formation of Hg film and then the formation of Cu−Hg intermetallic compound during the deposition process. As is well-known, the hanging mercury drop electrode (HMDE)[40,41] and mercury film electrode[2,42,43] have been widely used to enhance the sensitivity in heavy metal ions detection. Thus, the formation of Hg film and followed by the Cu−Hg intermetallic compound on the surface of SnO_2/graphene nanocomposite improve the sensitivity toward Cu(II). During simultaneous analysis of Cd(II), Pb(II), Cu(II), and Hg(II), the sensitivity obtained was 18.4, 18.6, 14.98, and 28.2 $\mu A\,\mu M^{-1}$, respectively. We find that both sensitivities of Cu(II) and Hg(II) increased significantly, but with relative low correlation coefficients (as shown in Figure 7), in comparison with the individual and simultaneous analysis of Cu(II) and Hg(II). We considered that this result could also be explained by the intermetallic compounds formed among the four target metal ions and the competition for the limited number of active sites at the modified electrode surface, even though the actual reason for how these ions exert their effects on each other is unclear at the present stage.

For a better understanding of the enhancement in sensitivity for Cu(II) and Hg(II) when analyzed simultaneously, we further studied the effect of the concentrations of Cd(II) or Pb(II) on the anodic peak currents of Cu(II) and Hg(II). Figure 8a reveals the SWASV response of the SnO_2/graphene nanocomposite electrode at different concentrations of Cd(II) in the presence of 0.5 μM Cu(II) and 0.5 μM Hg(II), showing the interference of the concentrations of Cd(II) on the anodic peak currents of Cu(II) and Hg(II). Combining Figure 8, parts a with b, it can be observed that with the addition of 1.0 μM Cd(II), the peak current of Cu(II) increased slightly while the peak current of Hg(II) significantly increased. Then, with the further addition of Cd(II), the peak currents of Cu(II) and Hg(II) tended to level off. This result was likely due to the formation of Cd film and followed by the formation of Cd−Cu[35] and Cd−Hg[39] intermetallic compounds during the deposition step, which increased the sensitivity for Cu(II) and Hg(II). When the concentration of Cd(II) reached a certain high value, there may exist surface saturation for the formation of Cd film, thus the peak currents of Cu(II) and Hg(II) tended to level off.

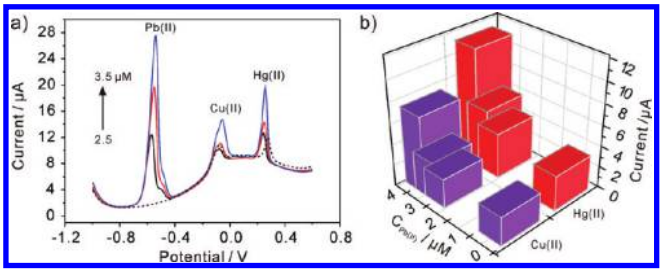

Figure 9. (a) SWASV response of the SnO_2/reduced graphene oxide nanocomposite modified GCE at 0, 2.5, 3.0, and 3.5 μM Pb(II) in the presence of 0.5 μM Cu(II) and 0.5 μM Hg(II) in 0.1 M NaAc-HAc (pH 5.0), showing the interference of the concentrations of Pb(II) on the anodic peak currents of 0.5 μM Cu(II) and 0.5 μM Hg(II). (b) Comparison of the voltammetric peak current of Cu(II) and Hg(II) at different concentrations of Pb(II) corresponding to panel a. SWASV conditions are identical to those in Figure 3.

Similarly, the SWASV response of the SnO_2/graphene nanocomposite electrode at different concentrations of Pb(II) in the presence of 0.5 μM Cu(II) and 0.5 μM Hg(II) was studied (Figure 9), It can be observed that with the addition of Pb(II), the peak currents of Cu(II) and Hg(II) almost remain the same at first. However, when the concentration of Pb(II) reached a certain high value, the peak currents of both Cu(II) and Hg(II) significantly increased. In addition, a slight shift for the peak of Hg(II) was observed. Similarly, this result was likely due to the formation of Pb film and followed by the formation of Pb−Cu[36] and Pb−Hg[39] intermetallic compounds during the deposition step, which increased the sensitivity for Cu(II) and Hg(II). At low Pb(II) concentration, there are not enough Pb(II) ions to create the film. Hence, when measurements are carried out at higher Pb(II) concentration, the significant increase of analytical signals was observed.

Hg film has generally been used to enhance the sensitivities of other target metal ions in heavy metal ion detection. However, the extreme toxicity and environmentally hazardous nature of mercury restricted the use of mercury electrodes for disposal and on-site analysis.[44] Bismuth nanoparticles were developed for determination of metal ions, such as Cd(II) and Pb(II), instead of mercury due to its ability to form "fusible" alloys and amalgams with the analyte metals.[45,46] On the basis of our results, we expect

that it is possible to use the Cd film or Pb film coated electrodes to enhance the detecting sensitivities toward Cu(II) and Hg(II).

4. CONCLUSIONS

In the present study, using SnO_2 nanoparticles with graphene for the simultaneous electrochemical determination of Cd(II), Pb(II), Cu(II), and Hg(II) was reported for the first time. The obtained results suggest that SnO_2/reduced graphene oxide nanocomposite is a promising material which possesses the advantages of both SnO_2 and graphene in electrochemically detecting heavy metal ions. The voltammetric peak for the stripping of Cd(II), Pb(II), Cu(II), and Hg(II) on the SnO_2/reduced graphene oxide nanocomposite electrode appears at different potentials with a separation of 212−480 mV between the stripping peaks. The described electrode can be used for the simultaneous detection of four heavy metals with a high stability and a long-term usage possibility. More significantly, an interesting phenomenon of mutual interference was also observed. We found that the presence of Cd(II) or Pb(II) could enhance the sensitivities toward Cu(II) and Hg(II). Thus, we expect that it is possible to use the Cd film or Pb film coated electrodes to enhance the detecting sensitivities toward Cu(II) and Hg(II) in further research. Despite some mutual interference effects, these ions can be reliably determined simultaneously. The obtained LOD were very well below the guideline value given by the World Health Organization (WHO). Finally, it could be shown that an expanded application of gas sensing material SnO_2 in stripping analysis of heavy metal ions is described in the present work, thus contributing the new sensing investigation for this nanostructured material.

AUTHOR INFORMATION

Corresponding Author

*Tel.: +86-551-5591142; Fax: +86-551-5592420; E-mail: wanglun@mail.ahnu.edu.cn (L.W); jhliu@iim.ac.cn (J.H.L); xingjiuhuang@iim.ac.cn (X.J.H).

ACKNOWLEDGMENT

This work was supported by the National Natural Science Foundation of China (21105073 and 21073197) and the National Basic Research Program of China (No. 2011CB933700). Y.W. thanks the State Key Laboratory of Environmental Chemistry and Ecotoxicology, Research Center for Eco-Environmental Sciences, Chinese Academy of Sciences (KF2011-18), and X.-J.H. acknowledges the One Hundred Person Project of the Chinese Academy of Sciences, China, for financial support.

REFERENCES

(1) Turyan, I.; Mandler, D. *Nature* **1993**, *362*, 703.
(2) Wu, H. P. *Anal. Chem.* **1996**, *68*, 1639.
(3) van Staden, J. F.; Matoetoe, M. C. *Anal. Chim. Acta* **2000**, *411*, 201.
(4) Bonfil, Y.; Brand, M.; Kirowa-Eisner, E. *Anal. Chim. Acta* **2002**, *464*, 99.
(5) Dai, X.; Nekrassova, O.; Hyde, M. E.; Richard, G. *Anal. Chem.* **2004**, *76*, 5924.
(6) Aragay, G.; Pons, J.; Merkoci, A. *J. Mater. Chem.* **2011**, *21*, 4326.
(7) Pumera, M.; Ambrosi, A.; Bonanni, A.; Chng, E. L. K.; Poh, H. L. *TrAC, Trends Anal. Chem.* **2010**, *29*, 954.
(8) Du, D.; Liu, J.; Zhang, X. Y.; Cui, X. L.; Lin, Y. H. *J. Mater. Chem.* **2011**, *21*, 8032.
(9) Williams, G.; Seger, B.; Kamat, P. V. *ACS Nano* **2008**, *2*, 1487.
(10) Xu, C.; Wang, X.; Zhu, J. *J. Phys. Chem. C* **2008**, *112*, 19841.
(11) Liu, J.; Fu, S.; Yuan, B.; Li, Y.; Deng, Z. *J. Am. Chem. Soc.* **2010**, *132*, 7279.
(12) Si, Y.; Samulski, E. T. *Chem. Mater.* **2008**, *20*, 6792.
(13) Gong, J. M.; Zhou, T.; Song, D. D.; Zhang, L. Z. *Sens. Actuators B-Chem.* **2010**, *150*, 491.
(14) Li, J.; Guo, S. J.; Zhai, Y. M.; Wang, E. K. *Anal. Chim. Acta* **2009**, *649*, 196.
(15) Li, J.; Guo, S. J.; Zhai, Y. M.; Wang, E. K. *Electrochem. Commun.* **2009**, *11*, 1085.
(16) Moses, P. R.; Wier, L.; Murray, R. W. *Anal. Chem.* **1975**, *47*, 1882.
(17) Jiang, L.-Y.; Wu, X.-L.; Guo, Y.-G.; Wan, L.-J. *J. Phys. Chem. C* **2009**, *113*, 14213.
(18) Yin, X. M.; Li, C. C.; Zhang, M.; Hao, Q. Y.; Liu, S.; Chen, L. B.; Wang, T. H. *J. Phys. Chem. C* **2010**, *114*, 8084.
(19) Song, H. J.; Zhang, L. C.; He, C. L.; Qu, Y.; Tian, Y. F.; Lv, Y. *J. Mater. Chem.* **2011**, *21*, 5972.
(20) Li, Y.; Lv, X.; Lu, J.; Li, J. *J. Phys. Chem. C* **2010**, *114*, 21770.
(21) Paek, S.-M.; Yoo, E.; Honma, I. *Nano Lett.* **2008**, *9*, 72.
(22) Fenghua, L.; et al. *Nanotechnology* **2009**, *20*, 455602.
(23) Bandura, A. V.; Sofo, J. O.; Kubicki, J. D. *J. Phys. Chem. B* **2006**, *110*, 8386.
(24) Hummers, W. S.; Offeman, R. E. *J. Am. Chem. Soc.* **1958**, *80*, 1339.
(25) Song, H.; Zhang, L.; He, C.; Qu, Y.; Tian, Y.; Lv, Y. *J. Mater. Chem.* **2011**, *21*, 5972.
(26) Meng, F. L.; Li, H. H.; Kong, L. T.; Liu, J. Y.; Z., J.; Jia, Y.; Liu, J. H.; Huang, X. J. *under review* **2011**.
(27) He, H.; Klinowski, J.; Forster, M.; Lerf, A. *Chem. Phys. Lett.* **1998**, *287*, 53.
(28) Lerf, A.; He, H.; Forster, M.; Klinowski, J. *J. Phys. Chem. B* **1998**, *102*, 4477.
(29) Wei, Y.; Yang, R.; Zhang, Y.-X.; Wang, L.; Liu, J.-H.; Huang, X.-J. *Chem. Commun.* **2011**, *47*, 5340.
(30) Yin, X. M.; Li, C. C.; Zhang, M.; Hao, Q. Y.; Liu, S.; Li, Q. H.; Chen, L. B.; Wang, T. H. *Nanotechnology* **2009**, 20.
(31) Teixeira Tarley, C. R.; Barbosa, A. F.; Gava Segatelli, M.; Costa Figueiredo, E.; Orival Luccas, P. *J. Anal. Atomic Spectr.* **2006**, *21*, 1305.
(32) Gao, X. H.; Wei, W. Z.; Yang, L.; Guo, M. L. *Electroanalysis* **2006**, *18*, 485.
(33) Pei, J. H.; Tercier-Waeber, M. L.; Buffle, J. *Anal. Chem.* **2000**, *72*, 161.
(34) Benbassat, A. H. I.; Azrad, A. *Electrochim. Acta* **1978**, *23*, 63.
(35) Grim, R. J. *J. Phys. Chem.* **1942**, *46*, 464.
(36) Tibbetts, D. F.; Davis, J.; Compton, R. G. *Fresenius J. Anal. Chem.* **2000**, *368*, 412.
(37) Alves, G. M. S.; Magalhaes, J.; Soares, H. *Electroanalysis* **2011**, *23*, 1410.
(38) Chan, H.; Butler, A.; Falck, D. M.; Freund, M. S. *Anal. Chem.* **1997**, *69*, 2373.
(39) Schiewe, J.; Oldham, K. B.; Myland, J. C.; Bond, A. M.; Vicente-Beckett, V. A.; Fletcher, S. *Anal. Chem.* **1997**, *69*, 2673.
(40) Sancho, D.; Vega, M.; Deban, L.; Pardo, R.; Gonzalez, G. *Analyst* **1998**, *123*, 743.
(41) Ferreira, M. A.; Barros, A. A. *Anal. Chim. Acta* **2002**, *459*, 151.
(42) Agra-Gutiérrez, C.; Ball, J. C.; Compton, R. G. *J. Phys. Chem. B* **1998**, *102*, 7028.
(43) Zen, J. M.; Lin, H. Y.; Yang, H. H. *Electroanalysis* **2001**, *13*, 505.
(44) Economou, A.; Fielden, P. R. *Analyst* **2003**, *128*, 205.
(45) Kachoosangi, R. T.; Banks, C. E.; Ji, X. B.; Compton, R. G. *Anal. Sci.* **2007**, *23*, 283.
(46) Toghill, K. E.; Wildgoose, G. G.; Moshar, A.; Mulcahy, C.; Compton, R. G. *Electroanalysis* **2008**, *20*, 1731.